Desalination and Water Treatment

Performance assessment of prepared polyamide thin film composite membrane for desalination of saline groundwater at Mersa Alam-Ras Banas, Red Sea Coast, Egypt

Moustafa M. Said [a], Abdel Hameed M. El-Aassar [a], Yousra H. Kotp [a], Hosam A. Shawky [a b] & Mohamed S.A. Abdel Mottaleb [c]

[a] Water Treatment & Desalination Unit, Desert Research Center, El-Matariya , Cairo , P.O.B 11753 , Egypt Phone: Tel. +2 01002930710 Fax: Tel. +2 01002930710

[b] Center of Nanotechnology, School of Engineering & Applied Sciences, Nile University , Smart Village-B 225 , Cairo , Egypt

[c] Faculty of Science, Ain Shams University , Cairo , Egypt
Published online: 30 May 2013.

PLEASE SCROLL DOWN FOR ARTICLE

Performance assessment of prepared polyamide thin film composite membrane for desalination of saline groundwater at Mersa Alam-Ras Banas, Red Sea Coast, Egypt

Moustafa M. Said[a], Abdel Hameed M. El-Aassar[a], Yousra H. Kotp[a], Hosam A. Shawky[a,b,*], Mohamed S.A. Abdel Mottaleb[c]

[a]*Water Treatment & Desalination Unit, Desert Research Center, El-Matariya, Cairo, P.O.B 11753, Egypt*
Tel. +2 01002930710; Fax: +2 0226389069; email: Shawkydrc@hotmail.com
[b]*Center of Nanotechnology, School of Engineering & Applied Sciences, Nile University, Smart Village-B 225, Cairo, Egypt*
[c]*Faculty of Science, Ain Shams University, Cairo, Egypt*

ABSTRACT

This study aims to enhance the performance of the flat sheet thin-film composite (TFC) polyamide–polysulfone reverse osmosis (RO) membranes. Composite RO membranes with high salt rejection were fabricated by treating a porous polysulfone (PS) support sequentially with a di-amine and then with a polyfunctional acid chloride, thereby forming a thin film of polyamide (PA) on the PS support. In order to establish conditions for the development of suitable thin-film composite (PS/TFC) membranes, various parametric studies were carried out which included varying the concentration of reactants, reaction time, curing temperature, and curing time for thin-film formation by the interfacial polymerization technique. By suitable combination of these factors, 2.0 wt.% MPD, 0.5 wt.% TMC, 60-s reaction time, 80°C curing temperature, and curing time 10 min., a desired thin film of PA with improved performance for groundwater desalination could be obtained. Further, a combination of scanning electron microscopy (SEM), attenuated total reflectance infrared (ATR-IR), X-ray diffraction (XRD) was utilized to confirm the existence and to examine the morphology of the PS/TFC membrane. Pilot-scale RO filtration unit was used to study the performance of the fabricated membranes for desalinating brackish, saline groundwater of Red Sea coastal area. Salt rejections percent for various feeds were found to be in the range of 90.6–98.5.

Keywords: Performance assessment; Brackish groundwater; Desalination reverse osmosis; Interfacial polymerization; Thin-film composite

---

*Corresponding author.

1. Introduction

Due to increasing demand for water, both potable and for irrigation, coupled with a decrease in suitable water sources, the shortage of drinking water becomes a major problem. In Egypt, desert region constitute more than 94% of the total area of the country. The other 6% of the area includes mainly the cultivated lands in Nile valley and Delta; on the other hand, the majority of Egyptian population is concentrated within the area of the Nile valley and Delta, whereas less than 5% of the population are scattered in all desert areas. The increasing population in Egypt and the limitation of the surface water resources (mainly Nile water) and, accordingly, the limitation of the cultivable lands in the Nile valley and Delta urged the successive governments to draw various programs for land reclamation in desert areas. Such programs, mostly, depend totally or partially on local groundwater resources in desert areas [1].

The area between Mersa Alam-Ras Banas, Red Sea coast of Egypt, is one of the driest areas in the world representing the eastern continuation of the Sahara Desert in North Africa. Water resources in such areas are mainly derived from groundwater and infrequent surface runoff, where water conservation projects are applied. The groundwater is considered as a major source of fresh water that is used in different purposes. However, most of groundwater in this area has water quality range from brackish to saline [2].

Desalination of brackish or saline water can potentially provide a new source of water by using highly mineralized water that would otherwise have little practical use. Supplies of brackish and saline groundwater within the area of study have the potential used to yield potable fresh water through desalination. Desalination is a water treatment process that converts brackish or saline water to fresh water by removing dissolved minerals (e.g. sodium and chloride ions) from the water, and where supplies of brackish or saline water exist, desalination can be used to yield potable fresh water.

Most widely applied and commercially proven desalination technologies fall into two categories of thermal (evaporative) and membrane-based methods. Membrane methods are less energy intensive than thermal methods and since energy consumption directly affects the cost-effectiveness and feasibility of using desalination technologies membrane methods, such as reverse osmosis (RO) and electro dialysis (ED), are attracted great attention lately. RO membrane has become one of the most efficient approaches for water purification, especially in successful applications for desalination of sea and brackish water, waste treatment and various separations in chemical, food, pharmaceutical, and other industries [3–6]. The concepts of "osmosis" and "reverse osmosis" have been known as early as 1,750 s. However, the use of RO as a feasible separation process is a relatively young technology since Loeb [7] developed a method for making asymmetric cellulose acetate membranes with relatively high water flux and separation. Moreover, the invention of thin-film composite (TFC) RO membrane was a milestone in the development of RO membrane [8,9]. Nowadays, the TFC membranes are widely used in commercial seawater desalination plants around the world, because they offer a combination of high flux and high selectivity unmatched by other types of RO membranes. As a result, the field of RO membranes has overwhelmingly moved in the direction of interfacial synthesized membranes, dominated by polyamide (PA) compositions. The active skin layer of PA plays the key role in TFC RO membranes, which controls mainly the separation property of the membrane, while the support layer gives the membrane necessary mechanical property [10–12]. A great advantage of TFC technology is that it allows development and successful handling of extremely thin layers of barrier materials formed from almost any conceivable chemical combination [13]. In addition, the ultra-thin barrier layer and the porous support can be independently optimized with respect to structure, stability, and performance.

This study focuses on the fabrication of brackish/ saline water polysulfone (PS)/thin film composite (TFC) RO membrane by *in situ* interfacial polymerization process. The structure of such prepared PS/TFC membrane was characterized by using FTIR, scanning electron microscopy (SEM), X-ray diffraction (XRD), and thermo-gravimetric analyzer (TGA). Moreover, this study aims to enhance the salt rejection and water flux of the synthesized PS/TFC membrane for brackish/ saline water desalination by optimizing interfacial polymerization conditions. Parametric studies were conducted by varying reaction time, monomer concentration, curing temperature, and time. The RO performance of the resulting fabricated membrane was evaluated in pilot-scale through permeation experiment of; firstly, synthetic water and secondly, brackish, saline, and sea water samples collected from the area located between Mersa Alam-Ras Banas, Red Sea of Egypt.

2. Experimental

2.1. Materials

PS pellets Udel P-3500 were supplied by Solvay, USA, N,N-dimethylacetamide (DMA) was supplied

from (Sigma-Aldrich). *m*-phenylenediamine (MPD), trimesoyl chloride (TMC), triethyl amine (TEA), (+)-10-champhor sulfonic acid (CSA), and sodium lauryl sulfate (SLS) were purchased from (Sigma-Aldrich). Other reagents such as n-hexane and sodium chloride (NaCl) were of analytical grade and used without further purification. Pure water with conductivity less than 5 µs/cm was produced by a two-stage RO system.

2.2. Water samples and analysis

Three water samples representing brackish, saline, and sea were collected from the area of study by the authors and analyzed in the field for temperature, pH, and specific conductance. Samples collected for cations and anions analysis were passed through 0.45-µm high-capacity filters and stored in polyethylene bottles. Cation samples were acidified in the field with ultra-pure nitric acid to a pH of <2. All samples were transported to the laboratory in ice-filled coolers and refrigerated at approximately 4℃ until analyzed. Fifty liters of water samples was also collected for the RO performance application.

Laboratory analyses for the collected water samples include the determination of EC, total dissolved salts (TDS), pH, concentration of major ions Ca^{2+}, Mg^{2+}, Na^+, K^+, CO_3^{2-}, HCO_3^-, SO_4^{2-} and Cl^-. Measurements were carried out by EC meter model Orion (150 A^+), pH meter (Jenway 3510), Flame photometer (Jenway PFP 7), Ion selectivity meter (Orion model 940 with 960 titration plus), UV/Visible spectrophotometer (Thermo-Spectronic 300), and inductively coupled plasma, (Thermo ICAP 6500). The obtained chemical data are expressed in milligram per liter (mg/l) or part per million (ppm).

2.3. Preparation of microporous PS support membrane

PS casting solution was prepared by dissolving 15 wt.% PS in DMA at 80–90℃ with continuous stirring. The resultant polymer solution was cast on a glass plate and gelled in a water bath. After 10 min of gelation, the resulting PS membrane was removed from the gelation bath and washed thoroughly with distilled water to remove the residual DMA. The membrane was then subsequently employed as a support medium for TFC membrane fabrication.

2.4. Fabrication of thin film composite membranes

The thin film coating was developed/fabricated to deposit the active skin layer of PA over the porous PS support membrane. Aromatic PA TFC RO membranes were made via the interfacial polymerization of MPD in aqueous phase and TMC in organic phase (n-hexane). CSA (4.0 wt.%), SLS (0.15 wt.%), and TEA (3 wt.%), were added into the aqueous phase. CSA and SLS were used to improve the absorption of MPD in microporous PS support membrane. TEA accelerated the MPD–TMC reaction by removing hydrogen halide formed during amide bond formation [13]. Firstly, the MPD solution was coated over the support membrane. The excess solution was carefully removed, and the membrane surface was dried. The MPD saturated support membrane was then immersed into the organic solution of TMC, followed by rinsing with n-hexane and heat curing. This resulted in the formation of ultra-thin aromatic PA film over the support membrane that was denoted as "nascent membrane" in this study. The nascent membranes could contain nascent aromatic PA (Fig. 1). The membranes were thoroughly washed and kept in deionized water before carrying out characterization or application studies.

2.5. Membrane characterization

Membrane samples used for the chemical and morphological structure analysis were washed with DI water and dried under vacuum before characterization. Attenuated total reflectance infrared (ATR-IR) characterization of the TFC RO membrane surface was made with a Nicolet avator 230 spectrometer at room temperature using Irtran crystal at 45° angle of incidence. Membrane morphology was examined by SEM Model Quanta FEG attached with EDX Unit. XRD was carried out using Shimadzu X-ray diffractometer, Model XD 490 Shimadzu, Kyoto (Japan) with a nickel filter and Cu-K_α radiation tube. Thermal stability of the obtained products was carried out using a Shimadzu DT-60H thermal analyzer, Shimadzu, Kyoto, Japan, from ambient temperature up to 1,000℃ with a heating rate of 10℃/min.

2.6. Performance test

RO performance for the synthesized PS/TFC membranes was conducted using ALFA LAVAL pilot-scale laboratory unit for membrane filtration model laboratory unit M20 (Fig. 2). A plate-and-frame unit is designed with open channels across the membrane surface. The feed stream/retentate flows through these. The membrane itself is supported by hollow plates with numerous slots that allow the permeate to collect and be removed from the unit via the permeate collecting tubes. Plate-and-frame units use the membrane itself, aided by lock rings or strips, to seal off
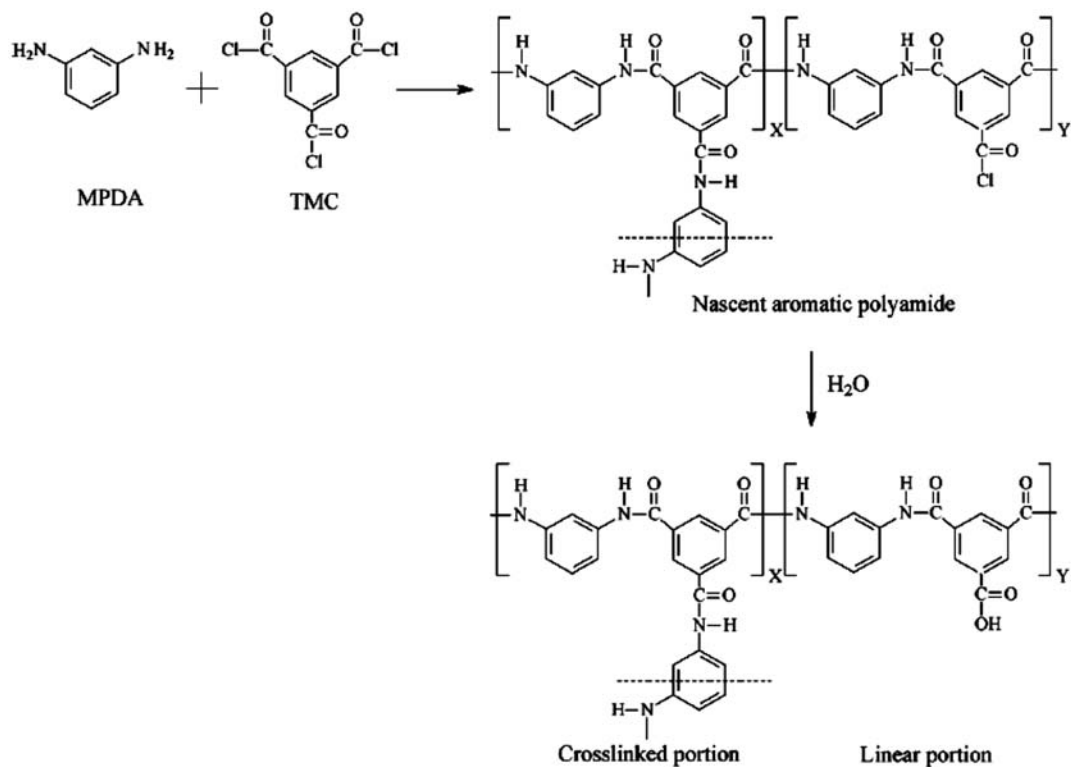
Fig. 1. Structure of PA skin layer formed by interfacial polymerization of MPD with TMC.
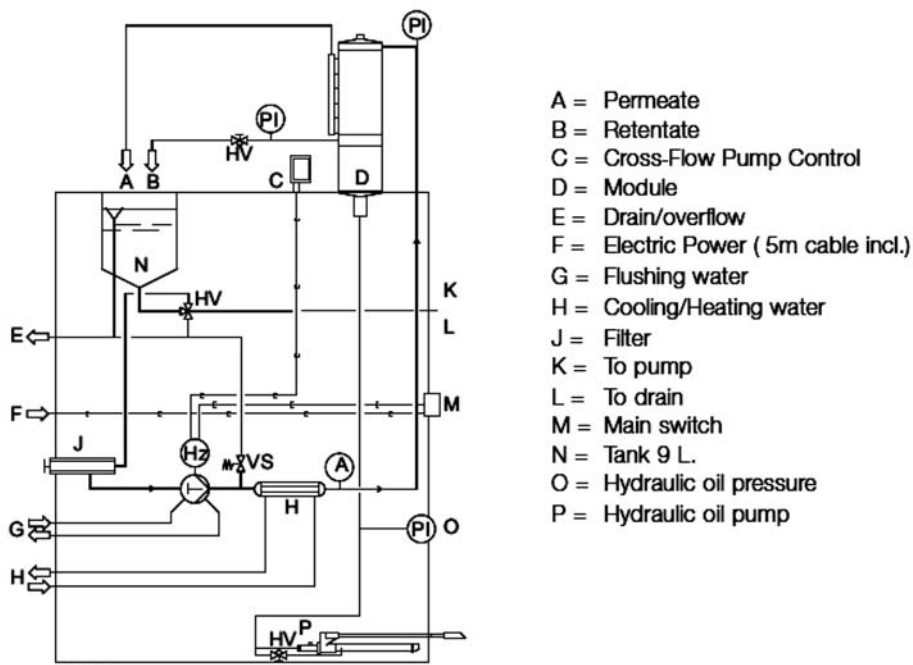
Fig. 2. Schematic diagram for Laboratory Unit 20 M pilot-scale membrane filtration.

the feed/retentate from mixing into the permeate channels. This also prevents any leaks from the plate stack itself. Flat-sheet membranes with effective area of 0.018 m² were placed in the test apparatus with the

active skin layer facing the feed water. All tests for TFC RO membranes performance were conducted at 12 bar (unless otherwise) using 6,000 ppm NaCl solution. Moreover, the RO desalination performance characteristics of the fabricated PS/TFC membrane were conducted for the three water samples collected from the area of study. All membrane samples were prepared and tested at least twice with a total of two membranes tests for RO performance, results of which have been averaged. The permeating volume collected for 1 h was used to describe flux in terms of liter per square meter per hour (L/m²h). A standardized conductivity meter was used to measure the salt (NaCl) concentrations in the feed and product water for determining membrane selectivity as given below:

Salt rejection $(\%) = [1 - C_p/C_f] \times 100$, where C_f and C_p are feed and permeating concentration, respectively.

3. Results and discussion

3.1. Spectroscopic characterizations of the PS support layer and the TFC membrane

Surface functional groups of modified PS support layer were characterized by ATR-FTIR. ATR-FTIR spectroscopy can provide a convenient and effective way to determine the composition of outmost part in a thin film composite RO membrane. It was performed in this study to confirm the successful preparation of thin film of PA onto PS support membrane surface. Thus, in the case of PS membrane, the FTIR spectrum (Fig. 3(a)) shows band at 835 due to the in-phase out-of-plane hydrogen deformation of para-substituted phenyl groups [14], band at 741 cm⁻¹ due

to aromatic hydrogen, three neighboring, band at 1,238 cm⁻¹ associated with the C–O–C asymmetric stretching vibration of the aryl–O–aryl group in PS [14], and those in the 1,294 and 1,149 cm⁻¹ regions are assignable to the asymmetric SO_2 stretching vibration and symmetric stretching vibration, respectively. In addition, the peak at 3,098 cm⁻¹ is due to O–H aromatic stretching and the peaks at ~1583.5 and 1,487 cm⁻¹ are associated with aromatic in-plane ring bend stretching vibration.

The spectrum of PS/TFC membrane is shown in Fig. 3(b), which indicates that the interfacial polymerization has occurred since the small band at 1,675 cm⁻¹(amide I) is present that is characteristic of C = O band of an amide group, C–N stretching, and C–C–N deformation vibration in a secondary amide group [15,16]. A strong peak at 1,736 cm⁻¹ assigned to C–O stretching (acid). In addition to this, other bands characteristic of PA are also seen at 1,544 cm⁻¹ (amide II, C–N stretch), the bands from 1,039–1,236 cm⁻¹ are characteristic of C–N bending and 1,487 cm⁻¹ (aromatic ring breathing), 858 cm⁻¹ (aromatic hydrogen, isolated) and 781 cm⁻¹ (aromatic hydrogen, three neighboring). Also, the stretching peak at 3,372–3474 cm⁻¹ can be assigned to N–H (and O–H) and suggests several loose associative features like NH….. N hydrogen bonds as also NH…O = C hydrogen bonds [17] and peak at 3,095.4 cm⁻¹ assigned to O–H aromatic stretching bands.

Surface characterizations of PS and PS/TFC membrane were evaluated by XRD, as shown in Fig. 4. XRD is used to investigate the change in the crystalline and noncrystalline nature of PS that may occur during the formation of TFC membrane. The characteristic diffraction peak for pure PS is observed at 2θ value of 18.00. The spectrum showed the highly
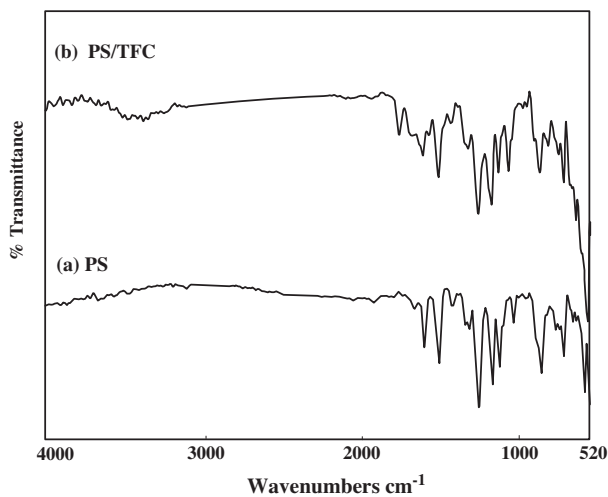

Fig. 3. ATR-FTIR spectra of (a) PS support layer and (b) thin film composite membrane.
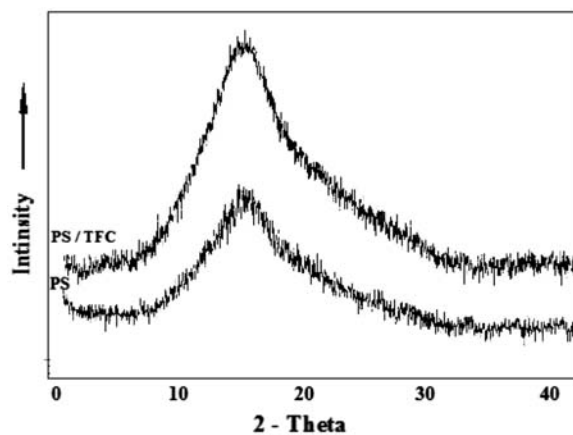

Fig. 4. XRD images of PS and thin film composite membrane.

amorphous nature of PS [18]. The broad peak at 18.00 (2θ) indicated that slight crystallinity was present, while the diffraction peak of PS/TFC membrane is observed at 2θ value of 18.00. The curves of PS/TFC were broad with higher intensity centered on 18 of 2θ, which emphasize the semi-crystalline nature of the composite [19]. The presence of crystalline regions in the composite is attributed to the PA skin, whereas amorphous regions are due to PS. The broad peak center on each X-ray pattern was attributed to the average intersegmental distance of polymer chains [20].

3.2. Microscopic characterizations of the PS support layer and the PS/TFC membrane

Components of the PS/TFC membrane, before and after interfacial polymerization, were observed by SEM (Fig. 5). Fig. 5(a) presents a cross-sectional view of the porous PS layer before interfacial polymerization and showing that PS have a sponge–structured, which can support high pressure, while Fig. 5(b) shows a cross-sectional view of the TFC membrane that consists of two distinctive layers with a dense layer (TFC layer of around 100 nm thickness) coated on top of the porous layer.

3.3. Thermal properties of the PS and PS/TFC membrane

Thermo gravimetric analysis (TGA) of PS and PS/TFC membranes were performed under nitrogen atmosphere as shown in Fig. 6. In both PS and PS/TFC membranes, there are two weight loss stages can be observed in the TGA curve (Fig. 6). The first stage at 451.4–561.97℃ and 304.70–551.94℃ for PS and PS/TFC, respectively, was taken as the splitting of –SO$_3$H.
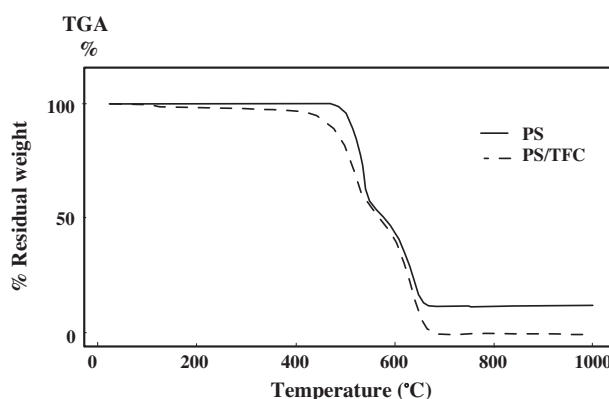

Fig. 6. TGA curves of PS and thin film composite membrane with the heating rate of 10℃/min.

In addition the weight loss is equal to 46.8 and 39.7% for PS and PS/TFC membranes, respectively, due to evaporation of additives (the boiling point of N,N dimethyl acetamide is 165℃) [21]. The second stage at above 729.9 and 760℃ is related to the splitting of the polymer main chain that accompanied by a weight loss equal to 41.92 and 58.15% for PS and PS/TFC membranes, respectively. It is noteworthy that the S = O group in the main chain of PS seems to form intermolecular hydrogen bonds with water. The weight loss of 58.15% occurs in PS/TFC membrane above 760℃ related to the splitting of the polymer main chain resulting in the final material carbon, which is obtained at more than 600℃. The reasons for such stability of PS/TFC membrane is expected to originate primarily from their chemical structure, which is composed of building units generally known to be highly resistant to increased temperatures, such as amide groups and aromatic moieties (benzene rings) [22].
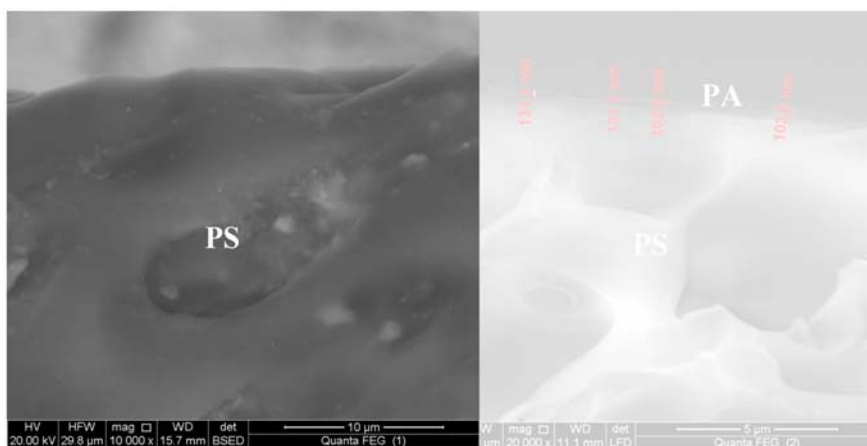

Fig. 5. Cross-section SEM images of: (a) PS support and (b) thin film composite membrane.

3.4. RO desalination performance optimization of the PS/TFC membrane

In general, the performance of the composite membrane is determined by the chemistry and the preparation conditions of the ultra-thin selective layer. In forming the thin-film, when the two monomer solutions are brought into contact, both monomers partition across the liquid–liquid interface and react to form a polymer; however, polymerization occurs predominantly in the organic phase due to the relatively low solubility of most acid chloride in water. Therefore, it is common to use a large excess of amine over acid chloride, which drives partitioning and diffusion of the amine into the organic phase [23,24].

In this study, different factors were studied to obtain the optimum condition necessary to prepare the best suitable PS/TFC membrane for desalination. Among the factors discussed are concentration of MPD monomer, concentration of TMC monomer, time of MPD impregnation, MPD-TMC reaction time, curing time, and temperature.

3.4.1. Concentration of MPD

Fig. 7 represents water flux and salt rejection of PF/TFC membrane prepared with different concentrations of MPD. It is observed form Fig. 7 that salt rejection increases with increasing MPD concentrations up to 2.0% and decreases at higher concentrations reflecting the existence of an optimum ratio between the concentration of MPD and TMC [25]. The presence of TEA in the aqueous MPD solution is necessary due to

its act as an acid acceptor and accelerates the MPD-TMC reaction by neutralizing hydrogen chloride producing during amide formation [26].

3.4.2. Concentration of TMC

Fig. 8 shows the performances of PS/TFC composite membranes prepared by different TMC concentrations. It can be seen from the figure that the salt rejection of the membrane increases from about 43 to 67%, whereas water flux decreases from about 12 to 5.5 L/m²h as TMC concentration increases. The observed salt rejection and water flux behavior of the membranes with increasing TMC concentration may be explained in terms of both the chemical and morphological changes that occur during the formation of PA skin layer. According to Morgan [27], at lower concentration of TMC monomer, the rate of polymerization is expected to be low because of the insufficient concentration of monomer at the interfacial reaction zone, and the formed selective skin layer is thin and loose; as a result, the membrane poorly rejects the salt but permeates more amount of water. For higher TMC concentrations, the rate of polymerization is faster and selective skin layer is somewhat thicker and compacter; thus, higher rejection and lower water flux can be expected for the membrane.

3.4.3. MPD impregnation time

The effect of different impregnation time in MPD aqueous solution on the water flux and salt rejection
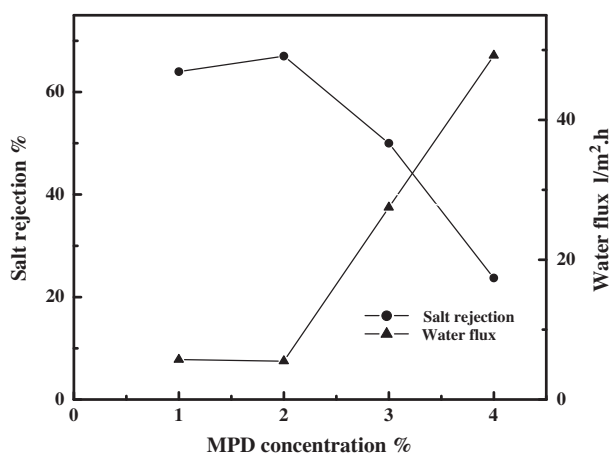

Fig. 7. Effect of MPD content in aqueous solution on salt rejection and water flux of the resulting PS/TFC membrane testing with 6,000 mg/l NaCl aqueous solution at 12 bar, 25℃ (TMC = 0.53 wt.%; reaction time 60 s; aqueous pH = 10.5; curing time = 10 min and curing temperature = 80℃).
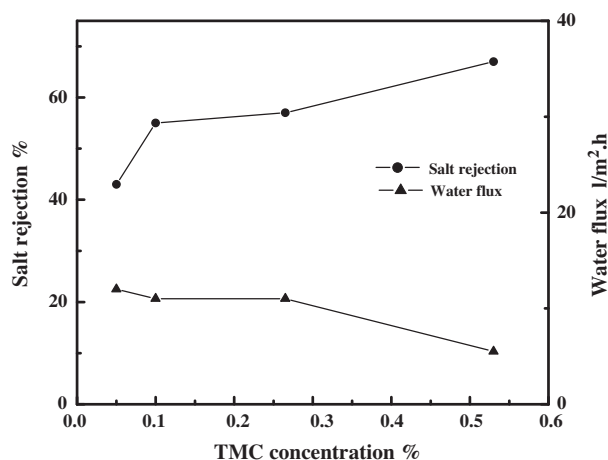
Fig. 8. Effect of TMC content on salt rejection and water flux of the resulting PS/TFC membrane testing with 6,000 mg/l NaCl aqueous solution at 12 bar, 25℃ (MPD = 2.0 wt.%; reaction time 60 s; aqueous pH = 10.5; curing time = 10 min and curing temperature = 80℃).

for the resulted PS/TFC membranes are presented in Fig. 9. According to the figure, at contact time between 1 and 2 min., the water flux and salt rejection seems to decrease and increase, respectively. On the other hand, for higher contact times, water flux increases and salt rejection decreases. A possible explanation is that for shorter times, not enough MPD has diffused into the surface of the support and for longer times too much has, and in both cases, the concentration in the surface of the support is not the optimum [25]. So a time of 2.0 min was selected for the further optimization of the other parameters.

3.4.4. MPD-TMC reaction time

Fig. 10 shows that salt rejection increases from 44 to 70% when MPD–TMC reaction time increases from 15 to 30 s, then rejection almost levels off when reaction time increase from 30 s up to 90 s. It is well known that the reaction time plays an important role in determining the extent of polymerization, and thereby the crosslinking and thickness of top skin layer as well as the resulting membrane performance [28,29]. Thus, for a short reaction time, the extent of crosslinking is low and the top skin layer is thin; as a result, the permeability of salt is high [30]. In this study, 60 s is considered as an optimal reaction time, which shows relatively high salt rejection and proper water flux.

3.4.5. Curing time and temperature

As shown in Fig. 11, the salt rejection increases with the curing time increasing from 5 to 10 min. With
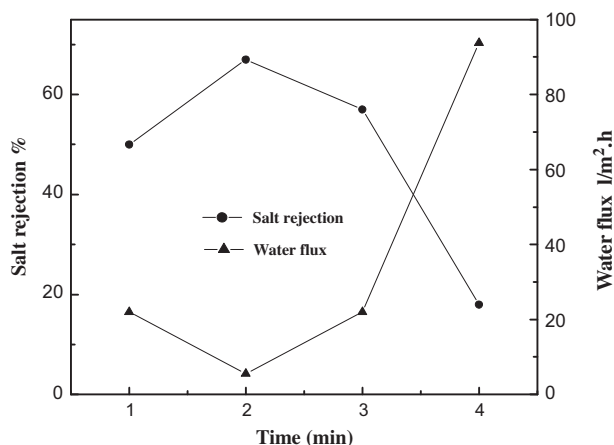
Fig. 9. Effect of MPD impregnation on salt rejection and water flux of the resulting PS/TFC membrane testing with 6,000 mg/l NaCl aqueous solution at 12 bar, 25°C (MPD = 2.0 wt.%; TMC = 0.53 wt.%; reaction time 60 s; aqueous pH = 10.5; curing time = 10 min and curing temperature = 80°C).
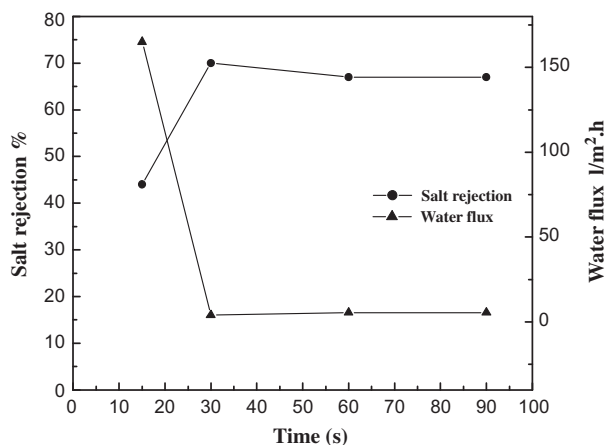
Fig. 10. Effect of interfacial reaction time on salt rejection and water flux of the resulting PS/TFC membrane testing with 6,000 mg/l NaCl aqueous solution at 12 bar, 25°C (MPD = 2.0 wt.%; TMC = 0.53 wt.%; aqueous pH = 10.5; curing time = 10 min and curing temperature = 80°C).

Fig. 11. Effect of curing time on salt rejection and water flux of the resulting PS/TFC membrane testing with 6,000 mg/l NaCl aqueous solution at 12 bar, 25°C (MPD = 2.0 wt.%; TMC = 0.53 wt.%; aqueous pH = 10.5; curing temperature = 80°C).

increase in curing time, the membrane is subjected to a prolonged exposure to curing temperature that results in pore shrinkage in the support membranes and the deeply densification of the skin layer [30].

Moreover, Fig. 12 shows increasing in salt rejection with the curing temperature increased from 65 to 80°C and drop off as the curing temperature is further increased. The increase in salt rejection at lower curing temperatures may be due to the increased densification or additional crosslinking of the selective skin layer and the loss of residual solvent in the film, respectively [31]. Whereby the decrease in salt
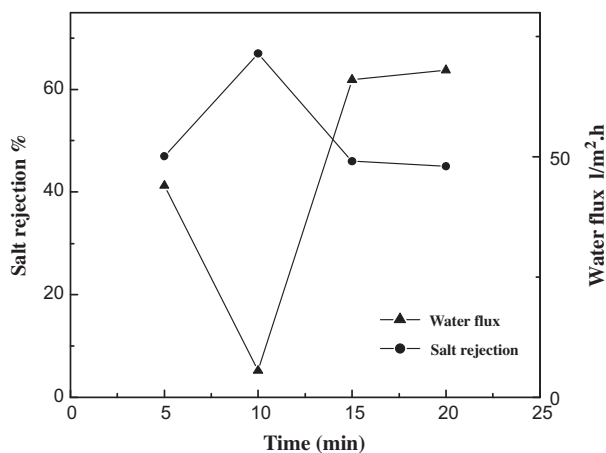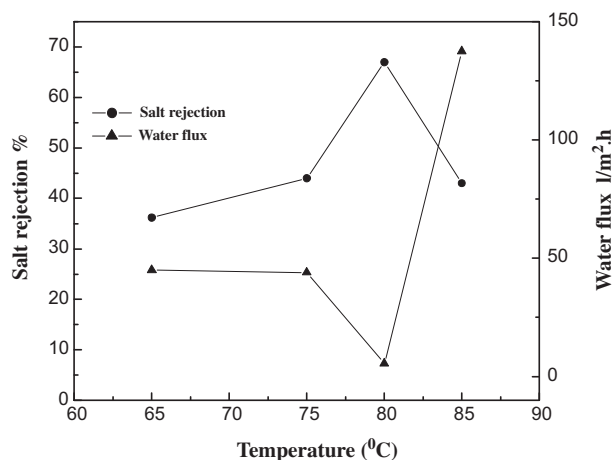
Fig. 12. Effect of curing temperature on salt rejection and water flux of the resulting PS/TFC membrane testing with 6,000 mg/l NaCl aqueous solution at 12 bar, 25°C (MPD = 2.0 wt.%; TMC = 0.53 wt.%; aqueous pH = 10.5; curing temperature = 80°C).

rejection at higher curing temperatures could be due to the pore shrinkage in the support membranes and the deeply densification of the skin layer [30].

3.5. Application of the fabricated PS/TFC composite RO membrane for groundwater desalination in Mersa Alam-Ras Banas area

Desalination of saline water and/or brackish groundwater by RO appears to be a sound option for arid lands bordering seas. Hence, there is a need in Egypt for capacity building of water desalination comprising technology transfer in membrane separation processes, operation and maintenance, and skilled

manpower [32]. For instance, desalination has been widely and successfully used in the Red Sea costal area.

From the aforementioned studies to the performance of different fabricated TFC membranes, it is clear that the best membrane possess have high salt rejection and water flux were achieved with the following conditions; 2.0 wt.% MPD, 0.5 wt.% TMC, 60 s reaction time, 80°C curing temperature and curing time 10 min. This membrane was selected for the desalination of three groundwater samples representing brackish, saline groundwater and Red seawater using RO pilot-scale laboratory unit (Laboratory Unit M20).

Table 1 shows the salt contents for the three water samples from which it can be seen that the salinity ranges from 8,022 to 39,775 mg/l. Such waters were pumped into the Laboratory Unit, M20 unit, at flow rate of 5 l/min, and operation pressure was applied using our fabricated selected membrane. Generally, desalination process must provide water of better quality. A summary of the water chemistry of the feeds and products for the three water samples area is presented in Table 1. From Table 1, it can be seen that the retention of bivalent ions is higher than that of monovalent ones and the retention for the bivalent anions is lower than that of cations. Moreover, the sequence of cations rejection (R%) is: R $Mg^{2+} > R$ $Ca^{2+} > R$ Na^+, while the sequence of anions rejection is: $RHCO_3^- > RSO_4^{2-} > RCl^-$. Thus, overall salt rejections % for various feeds were found to be in the range of 90.6–98.5. These results from Table 1 may be due to one or more of these factors; the first is ionic radii and hydrated ionic radii, where the hydrated ionic radii of divalent ions in solution are larger than

Table 1
Brackish, saline groundwater and Red Sea water characterization before and after desalination process

Analytical parameter	Na^+	K^+	Mg^{2+}	Ca^{2+}	HCO_3^-	SO_4^{2-}	Cl^-	TDS
Brackish water								
Feed (ppm)	1500.0	28.0	350.0	893.0	80.0	360.0	4851.0	8022.0
Product (ppm)	180	5.5	8	80	5	25	450	751
% Rejection	88	80.3	97.7	91	94	93	90.7	90.6
Saline water								
Feed (ppm)	2400.0	34.0	800.0	1700.0	150.0	1300.0	7700.0	15140.0
Product (ppm)	240	5	6	40	4	20	450	783
% Rejection	90	85	99	97.6	97.3	96.9	94.1	95
Red seawater								
Feed (ppm)	10750.0	500.0	1850.0	609.0	126.0	8966.0	17021.0	39775.0
Product (ppm)	180.0	4.5	10.0	15.0	2.0	100.0	270.0	580.0
% Rejection	98.3	99.1	99.4	97.5	99.2	98.8	98.4	98.5

that of monovalent ions [33–35]. The second is based on the different cationic valence rejection sequence that can be explained by the Donnan exclusion theory, which suggests that a higher valence counter ion caused a higher ion rejection, whereas a higher valence counter ion (neutral species) leads to a lower rejection of the salt [36]. For the same valence ions, the rejection sequence could be affected by the difference in ion diffusivities, that is, an ion is retained more if it has a smaller diffusivity this is inversely reflected in the rejection sequence [33]. The third is based on the interaction between the membrane surface and ions in solution. Those factors can explain the high rejection of Mg^{2+} and Ca^{2+} counter ions more than Na^+. The fourth is based on the hydration energy, where the difference of retention can be attributed to the difference of energy hydration between the divalent and monovalent ions; the more hydrated the divalent ions, the more difficult their transfer across the membrane, [37]. Consequently, SO_4^{2-} and HCO_3^- ions, which are more strongly hydrated than Cl^- ions, become difficult to permeate through the membrane.

4. Conclusions

Polymerization occurs almost simultaneously on liquid–liquid interface as MPD from water phase and TMC from organic phase contact each other. MPD quickly diffuses into organic phase and thus promotes the growth of membrane in the direction perpendicular to interface. Both structure and performance of PA membrane can be effectively controlled by adjusting reaction time and MPD and TMC concentrations. Membrane with flat surface morphology and uniform thickness can be prepared through this interfacial polymerization process. With controlled density and structure, the PA membrane with a thickness 100 nm can endow the PS/TFC membrane with selectivity 67% and water flux 5.5l/m^2.hr for 6,000 mg/l NaCl solution under 12 bar. Using this improved membrane for the desalination of brackish, saline groundwater, and Red seawater, the results showed that, the sequence of cations rejection ($R\%$) is: $R \ Mg^{2+} > R \ Ca^{2+} > R \ Na^+$, while the sequence of anions rejection is: $RHCO_3^- > RSO_4^{2-} > RCl^-$.

References

[1] M.G. Salim, Selection of groundwater sites in Egypt, using geographic information systems, for desalination by solar energy in order to reduce greenhouse gases, J. Adv. Res. 3 (2012) 11–19.

[2] A. Hafez, S. El-Manharawy, Economics of seawater RO desalination in the Red Sea region, Egypt. Part 1. A case study, Desalination 153 (2002) 335–347.

[3] M.A. Shannon, P.W. Bohn, M. Elimelech, J.G. Georgiadis, B.J. Marin, A.M. Mayes, Science and technology for water purification in the coming decades, Nature 452 (2008) 301–310.

[4] R.J. Petersen, Composite reverse osmosis and nanofiltration, J. Membr. Sci. 83 (1993) 81–150.

[5] D. Bhattacharyya, M.J. Evttch, J.K. Ghosal, J. Kozminsky, Reverse-osmosis membrane for treating coal-liquefaction wastewater, Environ. Prog. 3 (1984) 95–102.

[6] S. Lee, M. Elimelech, Relating organic fouling of reverse osmosis membrane to intermolecular adhesion forces, Environ. Sci. Technol. 40 (2006) 980–987.

[7] S. Loeb, The Loeb-Sourirajan membrane: How it came about, in: A. Turbak (Ed.), Synthetic Membranes, vol. I, ACS Symposium Series 153, Washington, DC, 1981.

[8] J.E. Cadotte, Interfacially synthesized reverse osmosis membrane, US Patent 4, 277, 344, 1981.

[9] J.E. Cadotte, R.J. Petersen, R.E. Larson, E.E. Erickson, New thin-film composite seawater reverse-osmosis membrane, Desalination 32 (1980) 25–31.

[10] Ch.Y. Tang, Y.N. Kwon, J.O. Leckie, Probing the nano- and micro-scales of reverse osmosis membranes—A comprehensive characterization of physiochemical properties of uncoated and coated membranes by XPS, TEM, ATR-FTIR, and streaming potential measurements, J. Membr. Sci. 287 (2007) 146–156.

[11] J.R. McCutcheona, M. Elimelech, Influence of membrane support layer hydrophobicity on water flux in osmotically driven membrane processes, J. Membr. Sci. 318 (2008) 458–466.

[12] P.S. Singh, S.V. Joshi, J.J. Trivedi, C.V. Devmurari, A. Prakash Rao, P.K. Ghosh, Probing the structural variations of thin film composite RO membranes obtained by coating polyamide over polysulfone membranes of different pore dimensions, J. Membr. Sci. 278 (2006) 19–25.

[13] S.H. Kim, S.-Y. Kwak, T. Suzuki, Positron annihilation spectroscopic evidence to demonstrate the flux-enhancement mechanism in morphology controlled thin-film-composite (TFC) membrane, Environ. Sci. Technol. 39 (2005) 1764–1770.

[14] Sadtler, The Infrared Spectra Atlas of Monomers and P-3-N. Kwon and polymers: Sadtler Research Laboratories, 1980.

[15] G. Socrates, Infrared Characteristic Group Frequencies, Wiley-Interscience, 1994.

[16] J.O. Leckie, Hypochlorite degradation of crosslinked polyamide membranes II. Changes in hydrogen bonding behavior and performance, J. Membr. Sci. 282 (2006) 456–464.

[17] H.A. Shawky, Performance of aromatic polyamide RO membranes synthesized by interfacial polycondensation process in a water-tetrahydrofuran system, J. Membr. Sci. 339 (2009) 209–214.

[18] Rajangam Padmavathi, Rajendhiran Karthikumar, Dharmalingam Sangeetha, Multilayered sulphonated polysulfone/silica composite membranes for fuel cell applications, Electrochim. Act. 71 (2012) 283–293.

[19] S.K. Yong, W.L. Sang, Y.K. Un, S.S. Jyong, Pervaporation of water-ethanol mixtures through crosslinked and surface-modified poly(vinyl alcohol) membrane, J. Membr. Sci. 51 (1990) 215–226.

[20] Lei Li, Suobo Zhang, Xiaosha Zhang, Guodong Zheng, Polyamide thin film composite membranes prepared from 3,4,5-biphenyltriacyl chloride, 3,3,5,5-biphenyl tetraacyl chloride and *m*-phenylenediamine, J. Membr. Sci. 289 (2007) 258–267.

[21] Yi Feng Liu, Qin Chun Yu, Yi Hua Wu, Preparation and proton conductivity of composite membranes based on sulfonated poly(phenylene oxide) and benzimidazole, Electrochim. Act. 52 (2007) 8133–8137.

[22] S. Villar-Rodil, J.I. Paredes, A. Martınez-Alonso, J.M.D. Tascon, Atomic force microscopy and infrared spectroscopy studies of the thermal degradation of Nomex aramid fibers, Chem. Mater. 13 (2001) 4297–4430.

[23] V. Freger, Kinetics of film formation by interfacial polycondensation, Langmuir 21 (2005) 1884.

[24] P.W. Morgan, S.L. Kwolek, Interfacial polymerization 2. Fundamentals of polymer formation at liquid interfaces, J. Polym. Sci. Pt. A: Polym. Chem. 34 (1996) 531.

[25] S. Ver´ıssimo, K.V. Peinemann, J. Bordado, Thin-film composite hollow fiber membranes: An optimized manufacturing method, J. Membr. Sci. 264 (2005) 48–55.

[26] R.J. Petersen, Composite reverse osmosis and nanofiltration membranes, J. Membr. Sci. 83 (1993) 81–150.

[27] P.M. Morgan, Condensation Polymers: Interfacial and Solution Methods, Interscience, New York, 1965.

[28] A.L. Ahmad, B.S. Ooi, Properties–performance of thin-film composites membrane: Study on trimesoyl chloride content and polymerization time, J. Membr. Sci. 255 (2005) 67.

[29] A.W. Mohammad, N. Hilal, M.N. Abu Seman, A study on producing composite nanofiltration membranes with optimized properties, Desalination 158(1–3) (2003) 73.

[30] A.P. Rao, N.V. Desai, R. Rangarajan, Interfacially synthesized thin film composite RO membranes for seawater desalination, J. Membr. Sci. 124 (1997) 263–272.

[31] A.K. Ghosh, B.-H. Jeong, X. Huang, E.M.V. Hoek, Impacts of reaction and curing conditions on polyamide composite reverse osmosis membrane properties, J. Membr. Sci. 311 (2008) 34–45.

[32] O. Al-Jayyousi, Capacity building for desalination in Jordan: Necessary conditions for sustainable water management, Desalination 141 (2001) 169–179.

[33] L. Antropov, Electrochimie Theorique. Mir, Moscow, 1975.

[34] J. Schaep, C. Vandecasteele, A.W. Mohammad, W.R. Bowen, Modeling the retention of ionic components for different nanofiltration membranes, Sep. Purif. Technol. 22–23 (2001) 169–179.

[35] M. Khayet, J.I. Mengual, Effect of salt type on mass transfer in reverse osmosis thin film composite membranes, Desalination 168 (2004) 383–390.

[36] Jiu-Qing Liu, Xu Zhen-Liang, Xin-Hai Li, Yao Zhang, Ying Zhou, Zhi-Xing Wang, Xue-Jun Wang, An improved process to prepare high separation performance PA/PVDF hollow fiber composite nanofiltration membranes, Sep. Purif. Technol. 58 (2007) 53–60.

[37] A.W. Vandecasteele, W.R. Mohammad, Bowen, Modeling the retention of ionic components for different nanofiltration membranes, Sep. Purif. Technol. 22–23 (2001) 169–179.